Magnetic Resonance and Kinetic Studies of the Manganese(II) Ion and Substrate Complexes of the Catalytic Subunit of Adenosine 3′,5′-Monophosphate Dependent Protein Kinase from Bovine Heart†

Richard Neil Armstrong,‡ Hiroki Kondo, Joseph Granot, E. T. Kaiser,* and A. S. Mildvan*

ABSTRACT: The catalytic subunit of cAMP-dependent protein kinase from bovine heart binds Mn^{2+} very weakly ($K_D \geq 1$ mM) as determined by electron paramagnetic resonance and by the enhancement of the paramagnetic effect of Mn^{2+} on the longitudinal relaxation rate $1/T_{1p}$ of water protons. The presence of a nucleotide such as ADP or AMP-PCP causes the appearance of two tight Mn^{2+} binding sites per molecule of enzyme which enhance the effects of Mn^{2+} on $1/T_{1p}$ of water protons by factors (ϵ) of 4 to 7. Titration of the enzyme with ADP in the presence of excess Mn^{2+}, monitoring the increase in the enhancement factor, reveals 0.95 tight ADP binding sites per enzyme molecule. In the enzyme–ADP complex, the affinities of Mn^{2+} for the two binding sites are equal (K_D = 19 μM), while in the ternary complex of enzyme, ADP, and the heptapeptide substrate, Leu-Arg-Arg-Ala-Ser-Leu-Gly, and in the binary enzyme–AMP-PCP complex the affinities for Mn^{2+} at the two sites are unequal (K_{D1} = 6–10 μM; K_{D2} = 50–60 μM). The presence of the substitution-inert complex $Co^{3+}(NH_3)_4ATP$ causes the appearance of only one Mn^{2+} binding site on the enzyme (K_D = 130 μM, ϵ = 9.6), indicating that the tighter of the two Mn^{2+} binding sites in the E–ADP–peptide and E–AMP-PCP complexes is on the enzyme-bound nucleotide while the more weakly bound Mn^{2+} is partially or entirely on the protein. A kinetic study of the enzyme-catalyzed phosphorylation of the peptide substrate reveals both activation and 50-fold inhibition by Mn^{2+}. Analysis of the data assuming a rapid equilibrium kinetic scheme yields an activator constant (3 μM) and an inhibitor constant (29 μM) for Mn^{2+} comparable to the dissociation constants of Mn^{2+} from the nucleotide site (6–10 μM) and protein site (50–60 μM), respectively, as determined in the binding studies. These findings indicate that the nucleotide-bound Mn^{2+} activates, while the more weakly bound Mn^{2+} is inhibitory, due to direct or indirect effects on the active site. Analogous results, differing only quantitatively, are obtained with Mg^{2+}. Thus, by studies of the binding of Mg^{2+} in competition with Mn^{2+}, two Mg^{2+} binding sites (K_D = 1.6 mM) are detected on the E–ADP complex, one of which activates and the other of which inhibits fivefold, as suggested by kinetic studies. Interactions between the inhibitory Mn^{2+} site and the active nucleotide–Mn^{2+} site on the enzyme are detected as a mutual tightening of binding and as an increase in enhancement at the inhibitory site when the active site binds a metal–nucleotide complex. The kinetically determined K_m values of ATP (69 μM) and of Mn^{2+}–ATP (16 μM) are in good agreement with the dissociation constants of nucleotides (65–78 μM) and Mn^{2+}–nucleotides (21–30 μM), respectively, as determined in the binding studies. This agreement indicates active site binding of the nucleotides and supports the validity of the rapid equilibrium kinetic scheme for the Mn^{2+}-activated enzyme. The requirement for nucleotides for the tight binding of Mn^{2+} to the enzyme and the ability of the substitution-inert species $Co^{3+}(NH_3)_4ATP$ to bind to the nucleotide site suggest that the coordination scheme of the active ternary complex is a nucleotide bridge or enzyme–ATP–metal complex.

Protein phosphorylation by adenosine 3′,5′-monophosphate dependent protein kinase (EC 2.7.1.37; ATP:protein phosphotransferase) is the major pathway by which cAMP[1] influences cellular metabolism. The activation of the enzyme by cAMP is known to occur via a cAMP-promoted dissociation of the inactive holoenzyme tetramer into two active catalytic subunit monomers and a regulatory subunit dimer. The specificity of the catalytic subunit for peptide and protein substrates has been studied (Zetterquist et al., 1976; Kemp et al., 1977), and though the enzyme is known to utilize ATP in preference to other nucleoside triphosphates (Walsh & Krebs, 1973) and to require a divalent cation for activity, most of the mechanistic details of the phosphoryl transfer are unknown.

The requirement for a divalent cation (Mg^{2+}) is well established (Krebs, 1972; Walsh & Krebs, 1973), but most metal ion studies have been qualitative and thus little is known about the detailed nature of this requirement. The proposed kinetic mechanisms (Moll & Kaiser, 1976; Pomerantz et al., 1977) for protein and peptide phosphorylation have not considered the catalytic role of the divalent cation through use of saturating or optimal magnesium ion concentrations. It has been reasonably assumed that the enzyme requires Mg^{2+} to form the substrate complex MgATP (Krebs, 1972). Indirect kinetic evidence (Moll & Kaiser, 1977) obtained with the bovine brain enzyme is consistent with this proposal as is a large body of evidence for many other phosphoryl transfer enzymes (Mildvan, 1970).

Some early kinetic investigations of cAMP-dependent (Huiging & Larner, 1966) and -independent (Gold & Segel, 1974) protein kinases suggested that a second metal ion might

† From the Departments of Chemistry (R.N.A., H.K., and E.T.K.) and Biochemistry (E.T.K.), University of Chicago, Chicago, Illinois 60637, and the Fox Chase Cancer Center (J.G. and A.S.M.), Philadelphia, Pennsylvania 19111. *Received September 26, 1978; revised manuscript received December 6, 1978.* Supported by National Institutes of Health Research Grants GM 19037 (E.T.K.) and AM 13351 (A.S.M.), National Science Foundation Grant PCM-74-03739 (A.S.M.), National Institutes of Health Postdoctoral Fellowship GM 05516 (R.N.A.), and a Chaim Weizmann Fellowship (J.G.). Support for the computation was provided by National Institutes of Health Grant CA-22780 and by an appropriation from the Commonwealth of Pennsylvania to the Institute for Cancer Research.

‡ Present address: National Institute of Arthritis, Metabolism and Digestive Diseases, National Institutes of Health, Bethesda, MD 20014.

[1] Abbreviations used: cAMP, adenosine 3′,5′-monophosphate; AMP-PCP, adenylyl methylenediphosphate; $Co^{3+}(NH_3)_4ATP$, cobalt(III) tetraammino-β,γ-phosphate-ATP; DTT, dithiothreitol; $NaDodSO_4$, sodium dodecyl sulfate; Tris, 2-amino-2-(hydroxymethyl)-1,3-propanediol; PRR, proton relaxation rate of water.

0006-2960/79/0418-1230$01.00/0

participate as an essential or nonessential activator. On the other hand, substitution of other divalent cations for magnesium or the use of high metal ion concentrations have been shown to inhibit the transferase activity (Moll & Kaiser, 1977; Berglund et al., 1977; Sugden et al., 1976; Miyamoto et al., 1969). While this inhibition has been variously explained as specific divalent metal ion inhibition or as an ionic strength effect (Moll & Kaiser, 1977), a clear interpretation has thus far not been possible due to the complex nature of the protein substrates used and the lack of quantitative data.

The present study was undertaken to clarify the role of divalent metal ions in the mechanism of protein phosphorylation by the catalytic subunit of bovine heart protein kinase. The interaction of Mn^{2+} with the catalytic subunit of protein kinase in the presence of various nucleotides and a peptide substrate was investigated by electron and nuclear magnetic resonance and kinetic techniques. A more limited study was made with Mg^{2+}. This investigation has allowed the physical and kinetic detection of specific divalent cation activating and inhibitory sites in various enzyme–substrate complexes.

Experimental Section

Materials

Sephadex G-10, Sephacryl S-200, Blue-Sepharose CL-6B, and SP-Sephadex were obtained from Pharmacia. CM-cellulose (CM-32) was from Whatman, Inc. β,γ-Methylene-ATP was purchased from Miles Laboratories. [γ-^{32}P]ATP was from Amersham/Searle. ADP was purchased from Sigma. All other compounds were reagent grade or the purest commercially available.

Preparation of Catalytic Subunit. The catalytic subunit of cAMP-dependent protein kinase from bovine heart muscle was prepared by the method of Demaille et al. (1977) with the following modifications. Ground heart muscle was homogenized once with 1.8 vol of extraction buffer. After centrifugation of the homogenate and collection of the supernatant, the pellet was resuspended with mild homogenation in 0.7 vol of buffer and centrifuged, and the supernatant was pooled with the first extract. This double-extraction procedure increased the final yield from ~15 to 35–40%. The enzyme obtained from the Blue-Sepharose CL-6B chromatography was concentrated to ~10 mL and chromatographed on a 2.6 × 90 cm bed of Sephacryl S-200 equilibrated with 50 mM Tris–150 mM KCl–0.1 mM DTT (pH 7.5). The enzyme obtained from this step was more than 98% homogeneous as judged by $NaDodSO_4$–gel electrophoresis and had a specific activity of 1400 μm/mg under standard assay conditions with protamine sulfate as substrate (Armstrong & Kaiser, 1978).

Preparation of $Co^{3+}(NH_3)_4ATP$. β,γ-Bidentate [Co^{3+}-$(NH_3)_4$ATP] was prepared and its structure established by ^{31}P NMR, as described by Cornelius et al. (1977). This racemic mixture of complexes, chiral at the β phosphorus, has two stereoisomers denoted as Δ and Λ (Merritt et al., 1978). The Δ isomer was separated from the mixture with hexokinase, as previously described (Cornelius & Cleland, 1978; Li et al., 1978).

Synthesis of Leu-Arg-Arg-Ala-Ser-Leu-Gly. The heptapeptide substrate was prepared by the solid-phase synthesis technique (Erickson & Merrifield, 1976). Protected (Boc) amino acids and Boc-Arg (NO_2) were obtained from Bachem. The peptide was grown on 1% cross-linked chloromethylated polystrene resin (Pierce Chemical Co.). The completed peptide was cleaved from the resin and deprotected by anhydrous hydrogen fluoride in the presence of anisole (Stewart & Young, 1968).

The crude peptide was purified by chromatography on a 2 × 90 cm bed of Sephadex G-10 in 1% acetic acid. The major fraction was lyophilized and chromatographed on a 2 × 35 cm bed of SP-Sephadex C-25 in 50 mM sodium acetate (pH 3.5). The peptide was eluted with a 700-mL linear gradient of 0–0.5 M NaCl. The major fraction was desalted by passage through Sephadex G-10, lyophilized, and applied to a 2 × 36 cm bed of CM-cellulose (Whatman CM-32) equilibrated with 25 mM ammonium acetate (pH 5.5). The peptide eluted as a single symmetric peak with a 1200-mL linear gradient of 25–250 mM ammonium acetate. The product was lyophilized to constant weight.

The final product gave an amino acid analysis of Ala (1.00), Arg (2.04), Gly (0.95), Leu (2.00), Ser (0.97) and showed a single N-terminal Leu residue (Hartley, 1970). The peptide migrated as a single spot on silica gel [acetic acid (3), 1-butanol (15), pyridine (10), and water (12), v/v, R_f 0.30] and CM-cellulose (50 mM KH_2PO_4, pH 5.0, R_f 0.15; 200 mM KH_2PO_4, pH 5.0, R_f 0.55) TLC. The peptide also migrated as a single spot on high-voltage paper electrophoresis at pH 9.1 (ammonium carbonate) and at pH 3.5 (pyridinium acetate). Maximal phosphorylation of the peptide led to the incorporation of 0.95 ± 0.15 mol of ^{32}P per mol of peptide.

Methods

Miscellaneous Methods. The concentration of the catalytic subunit was determined spectrophotometrically using $A_{280}^{1\%}$ = 14.9 (Demaille et al., 1977). Peptide concentration was determined by amino acid analysis after hydrolysis at 105 °C with 6 N HCl for 24 h. Values for Ser were corrected for 10% loss during hydrolysis. All kinetic and magnetic resonance studies were done in 50 mM Tris-Cl buffer at pH 7.5 in the presence of 150 mM KCl and 0.1 mM DTT. Substrate solutions used in the magnetic resonance experiments were passed through Chelex-100 (Bio-Rad) before use to remove paramagnetic contaminants.

Magnetic Resonance Measurements. The binding of Mn^{2+} to protein kinase was studied by two magnetic resonance methods as previously described (Cohn & Townsend, 1954; Mildvan & Engle, 1972). Electron paramagnetic resonance at 9.15 GHz with a Varian E-4 EPR spectrometer was used to monitor the free Mn^{2+} in a mixture of free and bound Mn^{2+} (Cohn & Townsend, 1954; Mildvan & Engle, 1972). The enhancement of the longitudinal relaxation rate ($1/T_1$) of water protons (PRR) at 24.3 MHz, using the spectrometer described elsewhere (Mildvan and Engle, 1972), monitored the effects of bound Mn^{2+}. The observed enhancement factor (ϵ^*) is defined as

$$\epsilon^* = \frac{1/T^*_1 - 1/T^*_{1,0}}{1/T_1 - 1/T_{1,0}} \quad (1)$$

where $1/T_1$ and $1/T_{1,0}$ represent the relaxation rates of water protons in the presence and absence of Mn^{2+}, respectively, and $1/T^*_1$ and $1/T^*_{1,0}$ represent the same parameters in the presence of protein kinase.

Analysis of Binding Data. The observed enhancement (ϵ^*) has previously been shown to be due to the weighted average of the enhancements due to all forms of Mn^{2+} (Mildvan & Cohn, 1963, 1966)

$$\epsilon^* = \sum_i \frac{[Mn^{2+}]_i}{[Mn^{2+}]_T}\epsilon_i \quad (2)$$

where $[Mn^{2+}]_i$ is the concentration of the ith complex of Mn^{2+}, $[Mn^{2+}]_T$ is the total Mn^{2+}, and ϵ_i is the enhancement factor of the ith complex of Mn^{2+}. The EPR and PRR data were

used to calculate the dissociation constants and enhancement factors ϵ_i for the various Mn^{2+} complexes studied.

The binding of Mn^{2+} and substrates to protein kinase was found in the present study to involve the formation of binary, ternary, and quaternary complexes. The dissociation constants for the relevant interactions in the systems under investigation are defined in eq 3. From their definitions the relationships

$$\begin{aligned} K(\text{E–S}) &= [\text{E}][\text{S}]/[\text{ES}] \\ K(\text{M–E}) &= [\text{M}][\text{E}]/[\text{ME}] \\ K(\text{S–M}) &= [\text{S}][\text{M}]/[\text{SM}] \\ K(\text{ES–M}) &= [\text{ES}][\text{M}]/[\text{ESM}] \\ K(\text{ME–S}) &= [\text{ME}][\text{S}]/[\text{MES}] \\ K(\text{E–S–M}) &= [\text{ME}][\text{S}]/[\text{ESM}] \\ K(\text{M–ES}) &= [\text{M}][\text{ES}]/[\text{MES}] \\ K(\text{E–SM}) &= [\text{E}][\text{SM}]/[\text{ESM}] \\ K(\text{M–E–S}) &= [\text{E}][\text{SM}]/[\text{MES}] \\ K(\text{M–ESM}) &= [\text{M}][\text{ESM}]/[\text{MESM}] \\ K(\text{ME–SM}) &= [\text{ME}][\text{SM}]/[\text{MESM}] \\ K(\text{MES–M}) &= [\text{MES}][\text{M}]/[\text{MESM}] \end{aligned} \tag{3}$$

among the equilibrium constants shown in eq 4 hold. Hence

$$K(\text{E–S})\cdot K(\text{ES–M}) = K(\text{M–E})\cdot K(\text{E–S–M}) = K(\text{S–M})\cdot K(\text{E–SM})$$

$$K(\text{ME–S})\cdot K(\text{MES–M}) = K(\text{E–S–M})\cdot K(\text{M–ESM}) = K(\text{S–M})\cdot K(\text{ME–SM}) \tag{4}$$

$$K(\text{M–E})\cdot K(\text{ME–S}) = K(\text{E–S})\cdot K(\text{M–ES}) = K(\text{S–M})\cdot K(\text{M–E–S})$$

only six of the dissociation constants are independent. [E], [S], and [M] represent the free concentrations of the enzyme, substrate, and metal ion; [ES], [ME], and [SM] are the concentrations of the binary complexes; [ESM] and [MES] are the concentrations of the ternary complexes where the metal ion binds either at the enzyme-bound substrate site or at a second site on the enzyme, respectively; and [MESM] is the concentration of the quaternary complex formed when both the metal sites are occupied.

The observed enhancement (eq 2) may be written as follows

$$\epsilon^* = \frac{[\text{M}]}{[\text{M}]_\text{T}} + \frac{[\text{SM}]}{[\text{M}]_\text{T}}\epsilon_\text{b}^{\text{SM}} + \frac{[\text{ME}]}{[\text{M}]_\text{T}}\epsilon_\text{b}^{\text{ME}} + \frac{[\text{ESM}]}{[\text{M}]_\text{T}}\epsilon_\text{t}^{\text{ESM}} + \frac{[\text{MES}]}{[\text{M}]_\text{T}}\epsilon_\text{t}^{\text{MES}} + 2\frac{[\text{MESM}]}{[\text{M}]_\text{T}}\epsilon_\text{q} \tag{5}$$

where $[\text{M}]_\text{T}$ is the total Mn^{2+} concentration. The enhancement of free Mn^{2+} is 1 by definition (eq 1). ϵ_b, ϵ_t, and ϵ_q are the enhancement factors of the binary, ternary, and quaternary complexes, respectively. The enhancement factor of the quaternary complex ϵ_q represents the average of the enhancements at each Mn^{2+} site when both sites are occupied.

In general, values of K(S–M) were obtained from the literature or were measured independently by EPR. A limiting value of K(M–E) was estimated from EPR data. Values of K(ES–M) and of K(M–ESM) were obtained from Scatchard analyses of Mn^{2+} titrations of the various ES systems using EPR. The values of K(E–S) and K(ME–SM) were determined by an iterative computer analysis of substrate titrations of the enzyme Mn^{2+} system, using PRR. Assuming neither cooperativity nor anticooperativity between the metal binding sites, K(ES–M) was taken as equal to K(MES–M) which, from eq 4, is equivalent to assuming that K(M–ES) = K·(M–ESM). The remaining dissociation constants could then be calculated from eq 4. In the computer analysis of the substrate titrations, the concentrations of the various Mn^{2+} complexes were calculated using the four independently determined dissociation constants and initial values for the two other dissociation constants to be determined, together with the known total concentrations of enzyme, substrate, and Mn^{2+}. The results for all the data points were substituted in eq 5 and were subjected to a least-squares analysis to yield the unknown enhancement factors.

The enhancement parameters $\epsilon_\text{b}^{\text{SM}}$ have previously been determined (Mildvan & Cohn, 1966). The same value was used for all of the nucleotides. Initial estimates of $\epsilon_\text{t}^{\text{ESM}}$ and ϵ_q were obtained by Mn^{2+} titration of ES systems using EPR and PRR. The computer search was carried out over a wide range of values of the dissociation constants until a best fit between the calculated and the measured enhancements was obtained. The quality of the fit was expressed by the reduced χ^2 value defined as follows

$$\chi^2_\text{red} = \frac{1}{N - N_\text{P}}\sum_{i=1}^{N}\frac{[\epsilon^*_i(\text{exptl}) - \epsilon^*_i(\text{calcd})]^2}{\epsilon^*_i(\text{calcd})} \tag{6}$$

where N and N_P are the number of data and calculated parameters, respectively. It should be noted that since predetermined or independently measured dissociation constants and enhancement factors were used as constant parameters in the data analysis, the number of unknown parameters varied only between 2 and 4, while the number of data points in a titration was three- to fivefold greater. Moreover, titrations were carried out over ranges of concentration of enzyme, Mn^{2+}, and substrate appropriate for determining the unknown dissociation constants.

Kinetic Measurements. The assay procedures previously described (Witt & Roskoski, 1975; Maller et al., 1978) were used with the following modifications. All kinetic experiments were carried out in triplicate at 25 °C for 30 s at pH 7.5 under identical buffer and salt concentrations as those used for the magnetic resonance studies. The catalytic subunit was diluted with buffer containing 0.5 mg/mL of BSA. Final enzyme concentration was 5–10 nM in an assay volume of 40 μL. Peptide concentration in all kinetic runs was fixed at 675 μM. This concentration was ~40-fold higher than the apparent K_m previously determined by others (Kemp et al., 1977). The enzyme was therefore saturated with peptide, allowing treatment of the kinetic data as those of a one-substrate reaction. Nonlinear kinetic functions were analyzed by nonlinear regression fitting of the experimentally determined rates to the appropriate rate expression.

Results

Binding Studies with Mn^{2+}

Mn^{2+} Binding to Protein Kinase in the Absence and Presence of Nucleotides. In the absence of nucleotides, the direct binding of Mn^{2+} (5–200 μM) to protein kinase (118.5 μM) was very weak ($K_\text{D} \geq 1$ mM) and nonstoichiometric ($n < 1$ Mn^{2+} bound per subunit) as determined by EPR and by the low observed enhancement ($\epsilon^* = 2.0 \pm 0.5$) of the paramagnetic effects of Mn^{2+} on $1/T_1$ of water protons. The addition of up to 1.6 mM of the heptapeptide substrate Leu-Arg-Arg-Ala-Ser-Leu-Gly produced no increase but rather a 21% decrease in the observed enhancement, suggesting that this substrate did not induce further binding of Mn^{2+} to the enzyme. However, the addition of 360 μM levels of the nucleotides ADP, AMP-PCP, or $Co^{3+}(NH_3)_4$ATP to solutions containing protein kinase (126 μM) and Mn^{2+} (87 μM) yielded

much larger observed enhancement factors of 5.8, 5.7, and 5.0, respectively. These values of ϵ^* indicate significant complexation of Mn^{2+} by the enzyme since binary Mn^{2+}–nucleotide complexes have ϵ^* values of ~1.6 (Mildvan & Cohn, 1966). Similarly, the addition of ATP (336 μM) to a solution containing enzyme (119 μM), Mn^{2+} (82 μM), and peptide (1.54 μM) increased ϵ^* by more than threefold from a value of 2.0 to a value of 6.7 for the equilibrium mixture. Hence, as previously found for certain other kinase enzymes (Mildvan, 1970) such as creatine kinase (O'Sullivan & Cohn, 1966), nucleotide substrates or analogues are necessary for the tight binding of Mn^{2+} to protein kinase. This point was studied directly by Mn^{2+} titrations of protein kinase in the presence of equivalent concentrations of various nucleotides.

Mn^{2+} Titrations of Protein Kinase–Nucleotide Complexes. To determine the stoichiometry, affinity, and enhancement factors for Mn^{2+}, in various enzyme–nucleotide–Mn^{2+} complexes, mixtures of the enzyme (122–126 μM) and nucleotides (100–112 μM) were titrated with $MnCl_2$ (30–1630 μM) measuring the free Mn^{2+} by EPR and the effects of the bound Mn^{2+} on the $1/T_1$ of water protons by PRR.

Since the enzyme catalyzes the slow hydrolysis of ATP (Armstrong et al., 1978), the first such titration was made with the protein kinase–ADP system. As indicated by a Scatchard plot of the EPR data (Figure 1), the enzyme–ADP complex binds 2.2 ± 0.2 Mn^{2+} ions with similar dissociation constants of 19 ± 3 μM. Under the experimental conditions, the major complexes formed in the titration are ESM, MES, and MESM. The simplest explanation consistent with the data of Figure 1 is that the dissociation constants at the two metal sites are equal and independent, i.e., K(ES–M) = K(MES–M) = K(M–ES) = K(M–ESM) = 19 μM.

Using the values of $[M]/[M]_T$ determined by EPR, the enhancement data were analyzed to yield a single average enhancement factor (ϵ_{bound}) for the bound Mn^{2+}. Equation 5 thus reduces to the following simple form

$$\epsilon^* = \epsilon_{bound} - \frac{[M]}{[M]_T}(\epsilon_{bound} - 1) \qquad (7)$$

which, on rearranging, gives

$$\epsilon_{bound} = \left(\epsilon^* - \frac{[M]}{[M]_T}\right) \Big/ \left(1 - \frac{[M]}{[M]_T}\right) \qquad (8)$$

In order to examine the effect of Mn^{2+} site occupancy on the enhancement factor, the calculated values for ϵ_{bound} were plotted against $[Mn]_b/[E]_T$ (Figure 1, inset), where $[Mn^{2+}]_b$ is the concentration of bound Mn^{2+} and $[E]_T$ denotes the total enzyme concentration. Linear extrapolation of the data toward zero occupancy yields a value of $\epsilon_{bound} \sim 4$, which may be assigned to the average enhancement factors of the ESM and the MES complexes. Since these complexes may form with similar affinities, they cannot be distinguished from one another. At a site occupancy of 2, the value of $\epsilon_{bound} \sim 6$ may be assigned to ϵ_q, the average of the enhancements at each site when both sites are occupied.[2] With no site–site interaction, ϵ_q is expected to equal $^1/_2(\epsilon_t^{EMS} + \epsilon_t^{MES})$ or ~4. The present value of ϵ_q may thus indicate an increase of the enhancement when both Mn^{2+} sites are occupied due to site–site interactions.

[2] It should be noted that the extrapolated values at zero occupancy can be regarded only as rough approximations since the extrapolation need not be linear. The ϵ_q values are, however, better estimates. A more precise estimate of the enhancement factors at both Mn^{2+} sites is given by the substrate titrations of Figure 6.

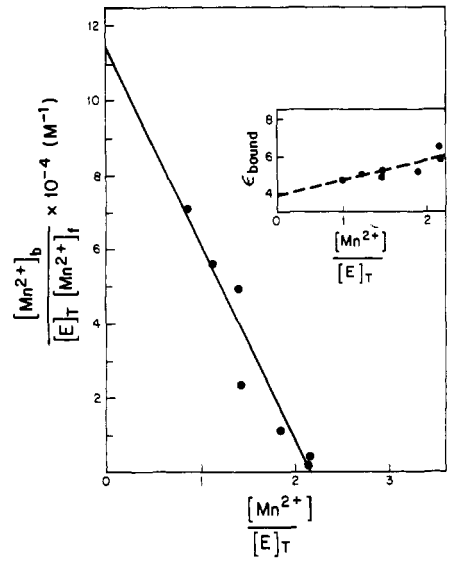

FIGURE 1: Scatchard plot of the binding of Mn^{2+} to the protein kinase–ADP complex. A solution containing ADP (111 μM) and the catalytic subunit of protein kinase (125 μM) was titrated with $MnCl_2$ (121–1630 μM). Other components present were 40 mM Tris-Cl buffer, pH 7.5, 0.12 M KCl, and 0.1 mM dithiothreitol. T = 22 °C. The theoretical curve was fitted to the data by a least-squares analysis with n = 2.2 sites per enzyme–ADP complex, with equal dissociation constants of 19 μM. $[E]_T$ denotes the total concentration of enzyme available for Mn^{2+} binding which is limited by the nucleotide concentration. The inset shows the enhancement of $1/T_{1p}$ of water protons at 24.3 MHz due to the bound Mn^{2+} as a function of Mn^{2+} site occupancy calculated with eq 8.

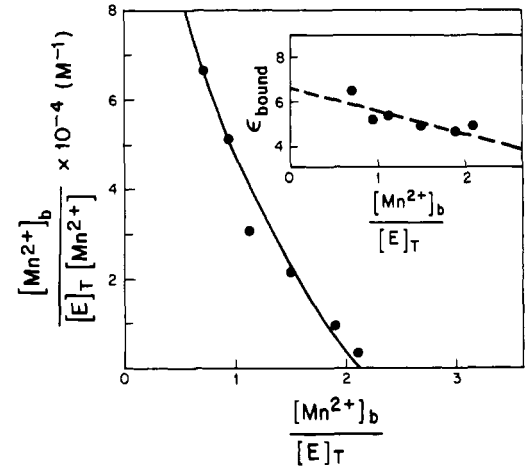

FIGURE 2: Scatchard plot of the binding of Mn^{2+} to the protein kinase–ADP–heptapeptide complex. A solution containing ADP (107 μM), the catalytic subunit (122 μM), and the heptapeptide substrate (770 μM) was titrated with $MnCl_2$ (85–1570 μM). The best-fit theoretical curve to the data points was obtained as previously described (Miziorko & Mildvan, 1974) with an average deviation of 11% by assuming 1.0 Mn^{2+} binding site with a dissociation constant of 10 μM and 1.1 Mn^{2+} binding site with a dissociation constant of 50 μM per enzyme–ADP–heptapeptide complex. Other components, conditions, and definitions are as given in Figure 1.

The progressive increase in ϵ_{bound} with occupancy may therefore be ascribed to an increase in the population of the complex containing two interacting Mn^{2+} ions. Further evidence for this interaction is presented below (Table I).

Saturation of the enzyme–ADP complex with the peptide substrate (950 μM) introduced significant curvature into the Scatchard plot (Figure 2) changing the affinities of the two Mn^{2+} binding sites in opposite directions, tightening one and weakening the other both by factors of ~2. The resulting dissociation constants were 10 ± 2 and 50 ± 10 μM (Table

Table I: Binding, Enhancement, and Kinetic Parameters of Protein Kinase, Mn^{2+}, Nucleotide Systems[a]

		binding studies				kinetic studies,
		ADP	ADP, peptide	AMP-PCP	$Co^{3+}(NH_3)_4ATP$[i]	ATP, peptide
A	K(E-S)	78	78	65 (120 ± 20)[g,h]	*b*	69 ± 9
	K(M-E)	1000	1000	1000	1000	
	K(S-M)	70[c]	70[c]	14[d]	~0.0	14[d]
	K(ES-M)	19 ± 3	10 ± 2	6.2 ± 1.2	~0.0	3.3 ± 0.6
	K(M-ESM)	19 ± 3	50 ± 10	60 ± 15	130	29 ± 9
	K(ME-SM)	0.4 (2.4 ± 0.8)[g]		1.8	39	
B	K(ME-S)	1.5		4.0	*b*	
	K(E-S-M)	1.5		0.4	*b*	
	K(M-ES)	19	50	60	*b*	
	K(E-SM)	21		30	301	16 ± 2
	K(M-E-S)	21		285	*b*	
	K(MES-M)	19	10	6.2	~0.0	
C	ϵ_b^{SM}	1.6[e]	1.6[e]	1.6[e]	*f*	
	ϵ_b^{ME}	8.0 ± 1.0	8.0 ± 1.0	8.0 ± 1.0	8.0 ± 1.0	
	ϵ_t^{ESM}	2.0 ± 1.0		2.5 ± 1.0	*f*	
	ϵ_t^{MES}	2.0 ± 1.0		6.5 ± 2.0	*f*	
	ϵ_q	6.7 ± 0.7	4.5 ± 1.5	7.0 ± 1.0	9.6 ± 1.0	
	χ^2_{red}	0.0015		0.0030	0.0001	

[a] The dissociation constants listed under A and the enhancement parameters listed under C were independently determined or directly evaluated by the computer analysis as described in Methods. The dissociation constants listed under B were calculated from those listed under A using eq 4. All dissociation constants are in μM. Where not indicated the uncertainties are approximately ±50%. [b] These dissociation constants cannot be defined for $Co^{3+}(NH_3)_4ATP$ because it is nondissociable. [c] From Jallon & Cohn (1970). [d] From Mildvan & Cohn (1966) assuming the equality of K(ATP-Mn^{2+}) and K(AMP-PCP-Mn^{2+}). Yount et al. (1971). [e] From Mildvan & Cohn (1966). [f] These enhancement parameters do not exist for the $Co^{3+}(NH_3)_4ATP$ complexes. [g] Values in parentheses were determined by equilibrium dialysis (Armstrong et al., 1979). [h] Value in parentheses determined for E-ATP complex. [i] With $Co^{3+}(NH_3)_4ATP$ the nucleotide-bound metal is fixed as Co^{3+} which is nondissociable. In the computer analysis, the formation of the higher complex $Co^{3+}(NH_3)_4ATP$-Mn^{2+} with a dissociation constant of 15 ± 5 mM was taken into consideration.

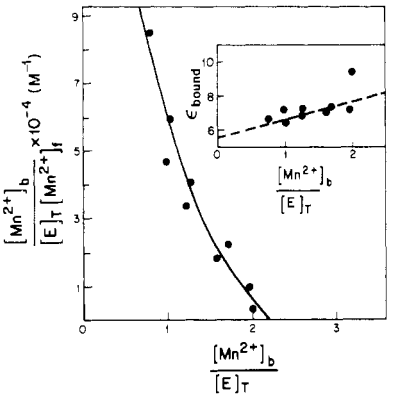

FIGURE 3: Scatchard plot of the binding of Mn^{2+} to the protein kinase–AMP-PCP complex. A solution containing AMP-PCP (100 μM) and the catalytic subunit (122 μM) was titrated with $MnCl_2$ (85–1570 μM). The best-fit theoretical curve to the data points was obtained as in Figure 2 with an average deviation of 13% by assuming 1.0 Mn^{2+} binding site with a dissociation constant of 6.2 μM and 1.2 Mn^{2+} binding sites with a dissociation constant of 60 μM per enzyme–AMP-PCP complex. Other components, conditions, and definitions are as given in Figure 1.

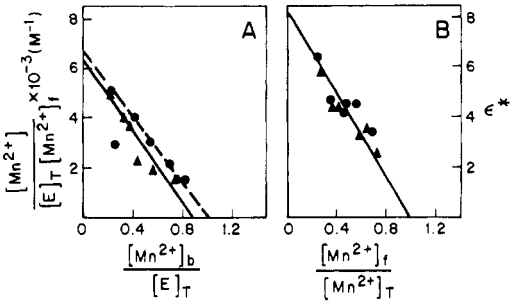

FIGURE 4: Mn^{2+} binding to the protein kinase–$Co^{3+}(NH_3)_4ATP$ complex. (A) Scatchard plot of the binding of Mn^{2+} (74–620 μM) to a solution containing the catalytic subunit (121 μM) in the presence of the Δ isomer (204 μM) (▲) or the racemate (443 μM) (●) of $Co^{3+}(NH_3)_4ATP$. Separate least-square lines were fitted to the data for the Δ isomer (n = 0.9 Mn^{2+} binding sites, dissociation constant = 120 μM) and for the racemate (n = 1.0 Mn^{2+} binding site, dissociation constant = 140 μM). (B) Plot according to eq 7 of the observed enhancement (ϵ^*) of $1/T_{1p}$ of water protons as a function of fraction of Mn^{2+} which is free, from the experiment in A. Other components, conditions and definitions are as given in Figure 1.

I). The enhancement data (Figure 2, inset) reveals an increase in the enhancement extrapolated to zero occupancy, i.e., ϵ_{bound} ~ 6.6. This value may be assigned to the enhancement factor of the tighter binding site for Mn^{2+} since this will be the first site to be occupied. At a site occupancy of 2, ϵ_{bound} ~ 4.5, indicating a decrease in ϵ_q with increasing occupancy. Hence the peptide inverts the effect of Mn^{2+} site occupancy on ϵ_{bound}. The data in the presence of the peptide do not distinguish between the presence or absence of an interaction between the two binding sites for Mn^{2+}.

As with ADP, the enzyme complex of the nonhydrolyzable β,γ-methylene analogue of ATP, AMP-PCP, also shows two Mn^{2+} binding sites, but with unequal dissociation constants of 6.2 and 60 μM (Figure 3). The enhancement data (Figure 3, inset) yield a value of ϵ_{bound} ~ 5.5 for site occupancy approaching zero, which may be again assigned to the enhancement factor of the tighter binding site. At a site occupancy of 2, ϵ_{bound} ~ 7.5, which is similar to the value obtained with ADP.

Hence, the binding of nucleotides to protein kinase causes the appearance of two tight Mn^{2+} binding sites, presumably one on the enzyme-bound nucleotide and the other on the enzyme itself. To test this point, the enzyme was titrated with Mn^{2+} in the presence of the substitution-inert metal–nucleotide complex $Co^{3+}(NH_3)_4ATP$. Under these conditions the nucleotide site is blocked by the nondissociable Co^{3+} ion. The Mn^{2+} titrations were carried out using either the resolved Δ isomer or a racemic mixture of the $Co^{3+}(NH_3)_4ATP$ stereoisomers. The Scatchard plots shown in Figure 4A indeed indicate only one binding site for Mn^{2+} with an average

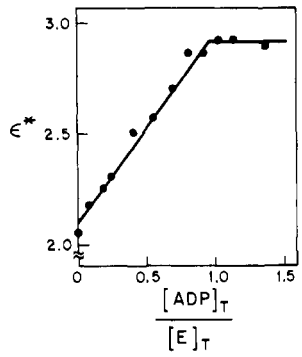

FIGURE 5: Determination of the number of ADP binding sites on the catalytic subunit of protein kinase. A solution containing enzyme (126 μM) and $MnCl_2$ (408 μM) was titrated with an otherwise identical solution which also contained ADP. Components and conditions are otherwise as described in Figure 1.

dissociation constant of 135 ± 30 μM with both the Δ isomer and the racemate. This high value suggests that the weaker of the two Mn^{2+} sites in the previous titrations is on the enzyme site while the tighter site is on the nucleotide. The enhancement data (Figure 4B) analyzed with eq 7 yielded the same enhancement factor (within the experimental uncertainty) of 9.6 ± 1.8 for the complexes of both the racemate and the Δ isomer. It thus appears that both isomers of this complex bind to protein kinase with similar affinity and structural effect. Verification of this conclusion was obtained by titrating a mixture of enzyme (86 μM) and Mn^{2+} (92 μM) either with the racemate or with the pure Δ isomer of $Co^{3+}(NH_3)_4ATP$. The titrations were essentially superimposable; that is, in both titrations the observed enhancement reached similar limiting values, at similar concentrations of the titrants.

Substrate Binding Studies. When a limiting level of protein kinase (126 μM) was titrated with ADP in the presence of excess Mn^{2+} (408 μM), a marked increase in ϵ^* was observed with a sharp end point at 0.95 ADP per enzyme molecule (Figure 5). The sharp and stoichiometric end point indicates tight 1:1 binding of the nucleotide to the enzyme.

To determine the dissociation constants and enhancement factors for the various species formed in the protein kinase–substrate–Mn^{2+} systems, lower concentrations of enzyme (33–39 μM) and Mn^{2+} (66.6 μM) were titrated with either ADP (5–54 μM), AMP-PCP (6-108 μM), or racemic $Co^{3+}(NH_3)_4ATP$ (5–181 μM). The data (Figure 6) were analyzed by computer as described in Methods using eq 3–5. As with the Scatchard analyses, the assumption was made that K(ES–M) = K(MES–M) or equivalently that K(M–ES) = K(M–ESM), i.e., that binding of a metal ion at one binding site does not affect the affinity for a metal ion at the second binding site. The best-fit parameters summarized in Table I were used to calculate the theoretical curves of Figure 6.

In the case of AMP-PCP (Figure 6B) the analysis was carried out with K(ES–M) = 6.2 μM and K(M–ESM) = 60 μM based on the data of Figure 3. The alternative assumption that K(M–ES) = 6.2 μM and that K(MES–M) = 60 μM yielded an identically good theoretical fit to the titration curve of Figure 6B (χ^2_{red} = 0.0030). Hence the data of Figure 6B alone do not permit a choice between these assumptions. However, on the basis of the results with $Co^{3+}(NH_3)_4ATP$, the former alternative seems more likely and has been assumed (Table I). Further support for this assignment is provided by the kinetic studies given below.

Inspection of Table I reveals that $Co^{3+}(NH_3)_4ATP$ binds to the enzyme significantly more weakly than do Mn^{2+}–nucleotide complexes. Independent measurements of K(E–ATP) and of K(MnE–ATPMn) by equilibrium dialysis (Armstrong et al., 1979) show reasonable agreement with the corresponding constants obtained by magnetic resonance (Table I).

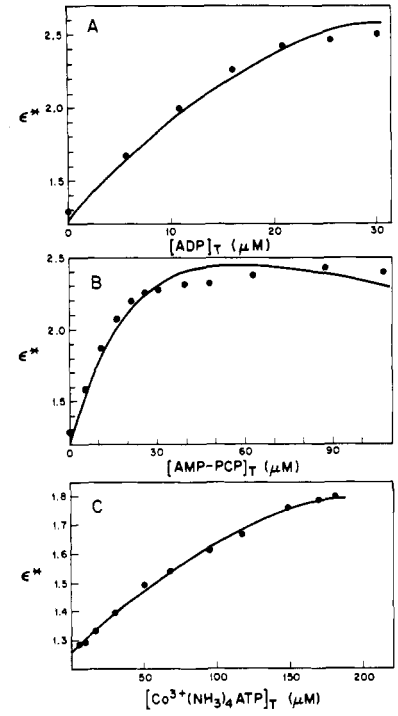

FIGURE 6: Nucleotide binding studies to the catalytic subunit of protein kinase. (A) ADP binding: a solution containing the catalytic subunit (33.2 μM) and $MnCl_2$ (66.6 μM) was titrated with an otherwise identical solution which also contained ADP. The theoretical curve fit to the data was computed from eq 5 using the parameters given in Table I. The components and conditions used in the binding of AMP-PCP (B) and the racemate of $Co^3(NH_3)_4ATP$ (C) are as in A and in Figure 1. The parameters used to fit the data are given in Table I.

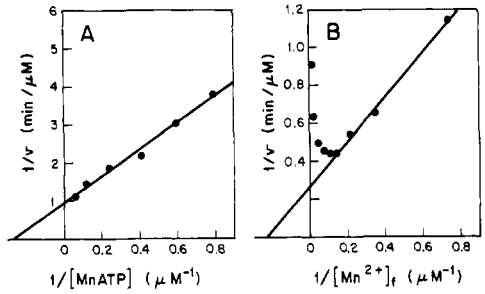

FIGURE 7: Effect of [MnATP] and $[Mn^{2+}]_f$ on the initial rates of peptide phosphorylation. (A) Double reciprocal plot of velocity vs. [MnATP]. $[Mn^{2+}]_T$ was fixed at 100 μM and [ATP] was varied from 1.5 to 20 μM with $[E]_T$ = 8.3 nM. Calculated kinetic constants are $K_{m(MnATP)}$ = 3.8 μM and k_{cat} = 127 min^{-1}. (B) Double reciprocal plot of velocity vs. $[Mn^{2+}]_f$ at fixed (98 μM) $[ATP]_T$. $[Mn^{2+}]_T$ was varied from 10 to 120 μM. Calculated kinetic parameters are $K_{A(Mn^{2+})}$ = 4.3 μM and k_{cat} = 416 min^{-1}. Solid lines are least-square fits to the data. $[Mn^{2+}]_f$ and [MnATP] were calculated assuming a metal–nucleotide dissociation constant of 14 μM.

The addition of nitrate (3–6 mM), an analogue of the transferred phosphoryl group (Milner-White & Watts, 1971; Reed & Cohn, 1972), to the dead-end complex of enzyme, MnADP, and peptide did not affect the enhancement, suggesting that nitrate does not bind or does not interact with the bound Mn^{2+}.

Kinetic Studies with Mn^{2+}

To clarify the role of Mn^{2+} and metal–nucleotide binding sites on protein kinase detected in the binding studies, a kinetic

$$v = \frac{\dfrac{k_1[E]_0[S][M]}{K_m(E\text{-}S)K_m(ES\text{-}M)} + \dfrac{k_2[E]_0[S][M]^2}{K_m(E\text{-}S)K_m(ES\text{-}M)K_I(M\text{-}ESM)}}{1 + \dfrac{[S]}{K_m(E\text{-}S)} + \dfrac{[S][M]}{K_m(E\text{-}S)K_m(ES\text{-}M)} + \dfrac{[S][M]}{K_m(E\text{-}S)K_I(M\text{-}ESM)} + \dfrac{[S][M]^2}{K_m(E\text{-}S)K_m(ES\text{-}M)K_I(M\text{-}ESM)}} \quad (9)$$

Scheme I[a]

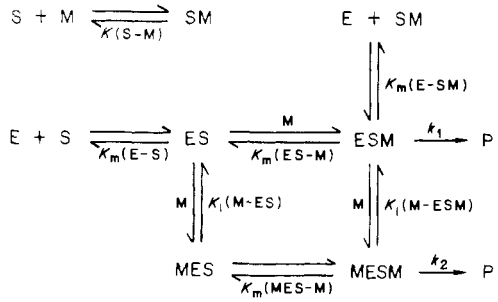

[a] E = enzyme-peptide complex, M = Mn^{2+}, S = ATP, and P = phosphorylated peptide.

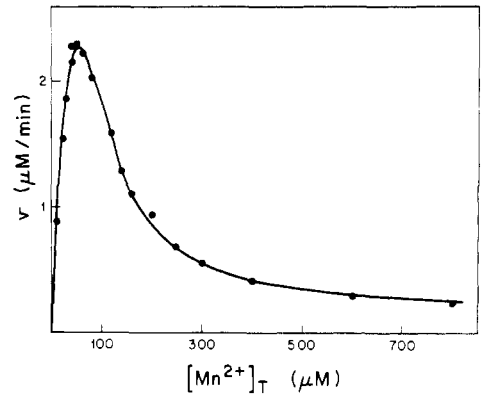

FIGURE 8: Typical dependence of the initial rate of peptide phosphorylation on total Mn^{2+} concentration. $[ATP]_T$ was fixed at 100 μM with enzyme at 8.9 nM. The solid line is a nonlinear regression fitting of the experimental points to the rate equation (eq 9) for Scheme I. Kinetic constants which define the line are found in Table II.

analysis of the Mn^{2+} activated enzyme was made. Initially, the kinetics of phosphorylation of the peptide substrate were studied under the limiting conditions of high and constant Mn^{2+} with variable ATP (Figure 7A) and of high and constant ATP with variable Mn^{2+} (Figure 7B). The reaction velocity has a simple hyperbolic dependence on [MnATP] yielding an apparent $K_{m(MnATP)}$ of 3.8 μM. In addition, at low concentrations of free Mn^{2+} the reaction exhibits a hyperbolic dependence on $[Mn^{2+}]_f$. The activator constant for Mn^{2+} of 4.3 μM is in reasonable agreement with the K(ES–M) values of the various nucleotides determined in the binding studies (Table I). The striking feature of Figure 7 is the marked inhibition of enzyme catalysis by free Mn^{2+}. The inhibition is manifest in Figure 7B at high $[Mn^{2+}]_f$ and is also obvious from the fourfold smaller apparent k_{cat} value obtained from Figure 7A where $[Mn^{2+}]_f \sim 95$ μM.

In order to study this inhibition in more detail the dependence of initial velocity on total Mn^{2+} concentration at several fixed ATP concentrations was examined. A typical kinetic experiment illustrated in Figure 8 satisfies, within experimental error of the data (~10%), a minimal kinetic scheme involving two Mn^{2+} binding modes (Scheme I). Using the rapid equilibrium assumption and the further assumption, analogous to that made in the binding studies, that K_m(ES–M) = K_m(MES–M), the rate equation (eq 9) was derived from Scheme I.

Figure 8 represents a typical computer fit of the experimental data to eq 9. The kinetic constants obtained from computer analysis of rate data obtained at three different ATP concentrations (Table II) show no dependence on the total ATP concentration as required by eq 9. That the MESM complex is catalytically active ($k_2 > 0$) is further supported by the observation of phosphoryl transfer catalysis at very high (10 mM) Mn^{2+} concentration. The K_m and K_I values obtained from the kinetic analysis (Table II) show good agreement with the dissociation constants of the corresponding unreactive complexes as measured in the binding studies (Table I). This agreement supports the validity of the rapid equilibrium assumption.

Kinetic and Binding Studies with Mg^{2+}

Magnesium, which is very likely the cation activator of protein kinase in vivo, activates and inhibits the catalytic subunit in a manner reminiscent of Mn^{2+} with estimated k_1(2000 min^{-1}) and k_2(400 min^{-1}) values fourfold and 60-fold

Table II: Kinetic Parameters Computed from the Manganous Ion Effect on Peptide Phosphorylation Rates[a]

	[ATP] (μM)			
constant	200	100	47	av
k_1, min^{-1}	450	650	420	510 ± 130
k_2, min^{-1}	5.5	12	3.6	7.0 ± 4.4
K_m(E–S), μM	65	63	80	69 ± 9
K_m(ES–M), μM	3.0	4.0	3.0	3.3 ± 0.6
K_I(M–ESM), μM	35	19	32	29 ± 9
K_m(E–SM),[b] μM	14	18	17	16 ± 2

[a] Values were obtained by nonlinear regression fitting of the experimental data to the rate equation for Scheme I assuming K(S–M) = 14 μM (Mildvan & Cohn, 1966). [b] These values were determined using the relationship K_m(E–S)K_m(ES–M) = K_m(E–SM)K(S–M).

greater, respectively, than with Mn^{2+}. Thus Mg^{2+} is a better activator and a less potent inhibitor of protein kinase than is Mn^{2+}. The quality of the theoretical fits to the kinetic data obtained in the presence of Mg^{2+} preclude an accurate determination of activator and inhibitor constants. Both of these constants, however, appear to be in the millimolar range.

The ability of Mg^{2+} to compete at the Mn^{2+} binding sites of protein kinase–nucleotide complexes was tested by magnetic resonance methods. A titration of the enzyme–Mn^{2+}–ADP complex with Mg^{2+}, measuring the enhancement of $1/T_1$ of the water protons (Figure 9), indicates the displacement of Mn^{2+} by Mg^{2+} from both of its binding sites. Considering only competition of Mg^{2+} for Mn^{2+} within the M–E–ADP–M complex and, for simplicity, neglecting the possible change in enhancement with Mn^{2+} site occupancy, a good fit to the data was obtained with dissociation constants for Mg^{2+} of 1.6 mM for both metal sites (Figure 9). A similar Mg^{2+} displacement experiment was carried out with the Mn^{2+}–E–Co^{3+}–$(NH_3)_4$ATP system. Analysis of the enhancement data (Figure 9) yielded a dissociation constant of 2.3 mM for Mg^{2+} from the Mg^{2+}–E–$Co^{3+}(NH_3)_4$ATP complex. These observations are in accord with the kinetic observations. As found with many other enzymes (Mildvan, 1970) the results with Mg^{2+} are qualitatively similar to but quantitatively different from those with Mn^{2+}.

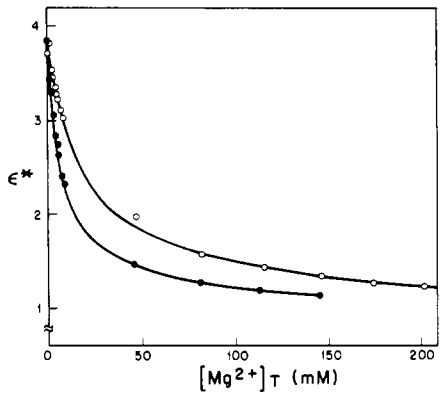

FIGURE 9: Displacement of Mn^{2+} from its enzyme–nucleotide complexes by Mg^{2+}. A solution containing either ADP (224 μM) (○) or racemic $Co^{3+}(NH_3)_4ATP$ (●), the catalytic subunit (126 μM), and $MnCl_2$ (204 μM) was titrated with $MgCl_2$ under conditions otherwise as described in Figure 1. The theoretical curve for the titration of the Mn^{2+}–enzyme–ADP–Mn^{2+} complex with Mg^{2+} was calculated by assuming n = 2.2 Mn^{2+} binding sites per mol of enzyme–ADP with equal dissociation constants of 19 μM (from the data of Figure 1) and the competitive binding of Mg^{2+} at both of these sites with equal dissociation constants of 1.6 mM. The theoretical curve for the titration of the Mn^{2+}–enzyme–$Co^{3+}(NH_3)_4ATP$ complex with Mg^{2+} was fit by assuming 1.0 Mn^{2+} binding site with a dissociation constant of 130 μM (from the data of Figure 4) and the competitive binding of Mg^{2+} at this site with a dissociation constant of 2.3 mM.

Discussion

The catalytic subunit of bovine heart protein kinase has one tight binding site for nucleotides as demonstrated by the sharp and stoichiometric end point found when the enzyme is titrated with ADP (Figure 5). The dissociation constants of nucleotides at this site (K[E–S]) are all similar and comparable to the kinetically determined K_m(E–S) for ATP, indicating this to be the active site. The similarity of the K(E–S) values of ADP, ATP, and AMP-PCP (Table I) implies that the γ-phosphoryl group does not play a significant role in nucleotide binding to the enzyme.

The binding of a nucleotide to the catalytic subunit causes the appearance of two tight Mn^{2+} binding sites which have dissociation constants that differ, at most, by an order of magnitude (Table I). When the substitution-inert metal–nucleotide complex $Co^{3+}(NH_3)_4ATP$ binds to the catalytic subunit, only one Mn^{2+} binding site, with a relatively high dissociation constant, appears. These findings indicate that when two Mn^{2+} binding sites of unequal affinity are observed, the tighter one is likely to be on the bound nucleotide. The apparent disappearance of one Mn^{2+} site with $Co^{3+}(NH_3)_4ATP$ and the three- to sixfold lower dissociation constant at the tight Mn^{2+} site with E–AMP-PCP and E–ATP as compared to E–ADP (Table I) suggest that the nucleotide-bound Mn^{2+} interacts with the polyphosphate chain.

The kinetic data allow the determination of the function of each metal binding site. In particular the Mn^{2+} which is more tightly bound is the essential metal ion activator while the more weakly bound Mn^{2+} is an inhibitor of catalytic activity (Table II). Moreover, the values of the activator (K_m(ES–M)) and inhibitor (K_I(M–ESM)) constants of Mn^{2+} are similar to the dissociation constants K(ES–M) and K(M–ESM), respectively. One may reasonably conclude that the activating metal is coordinated to the enzyme-bound nucleotide while the inhibiting metal binds to the enzyme–substrate complex.[3]

[3] Preliminary NMR studies of the Mn^{2+}–enzyme–$Co^{3+}(NH_3)_4ATP$ complex suggest that the inhibitory Mn^{2+} forms a bridge between the enzyme and the metal–nucleotide substrate.

Several lines of evidence suggest the coordination scheme of the active ternary complex to be a nucleotide bridge or E–ATP–Mn^{2+} complex as in hexokinase (Danenberg & Cleland, 1975) and creatine kinase (O'Sullivan & Cohn, 1966). First, nucleotides are essential for the tight binding of Mn^{2+} to the enzyme while Mn^{2+} produces only a two- to fourfold increase in the affinity of the enzyme for nucleotides. Second, $Co^{3+}(NH_3)_4ATP$, a substitution-inert complex which cannot acquire ligands from the enzyme, binds well to the nucleotide site. As suggested by the general agreement of the corresponding thermodynamic and kinetic parameters (Table I), the presence of the peptide substrate has only small effects on the dissociability and structure at the E–nucleotide–Mn^{2+} site.

The binding of Mn^{2+} at the inhibitory site markedly increases the affinity of the enzyme for nucleotides and metal–nucleotides at the active sites, typically, by two orders of magnitude. This effect may be symptomatic of or contribute to the profound inhibition caused by Mn^{2+}. Conversely, as mentioned above, the binding of nucleotides to the active site has a similarly large tightening effect on Mn^{2+} binding at the inhibitory site. Moreover, as manifested by changes in the enhancement parameters at the inhibitory site (i.e., ϵ_q always exceeds ϵ_t), the environment of the inhibitory site is altered by changing the ligands at the active site from nucleotide to metal–nucleotide. Clearly both the magnetic resonance and kinetic measurements indicate a strong mutual interaction between the inhibitory and active sites.[3]

The effects of the physiological activator Mg^{2+} are analogous to those found with Mn^{2+}. However, the inhibition by Mg^{2+} is much less pronounced than that observed with Mn^{2+} and for this reason it is questionable that Mg^{2+} plays any significant role in regulation of catalysis through interaction at the inhibitory metal site in vivo.

Although the precise location of the inhibitory site is at present unknown,[3] the fact that the site persists in the presence of a saturating level of peptide substrate and the incomplete inhibition by Mn^{2+} argue against the strict competition between Mn^{2+} and peptide binding. The relationships among the binding sites for the inhibitory Mn^{2+}, the regulatory subunit, and the peptide substrate are under further investigation.

Acknowledgments

We thank Professor J. H. Law for the use of a scintillation counter, Dr. D. J. Kroon for help with the peptide synthesis, J. Geever and Dr. C. D. Bossinger of the Armour Pharmaceutical Co. for performing the HF cleavage in the peptide synthesis, M. Schlieffer, Dr. M. Pring, and Dr. G. H. Reed for helpful advice in computing, and Maureen Fay for expert technical assistance.

References

Armstrong, R. N., & Kaiser, E. T. (1978) *Biochemistry 17*, 2840.

Armstrong, R. N., Kondo, H., & Kaiser, E. T. (1979) *Proc. Natl. Acad. Sci. U.S.A.* (in press).

Berglund, L., Ljungstrom, O., & Engstrom, L. (1977) *J. Biol. Chem. 252*, 613.

Cohn, M., & Townsend, J. (1954) *Nature (London) 173*, 1090.

Cornelius, R. D., & Cleland, W. W. (1978) *Biochemistry 17*, 3279.

Cornelius, R. D., Hart, P. A., & Cleland, W. W. (1977) *Inorg. Chem. 16*, 2799.

Danenberg, K. D., & Cleland, W. W. (1975) *Biochemistry 14*, 28.

Demaille, J. G., Peters, K. A., & Fischer, E. H. (1977) *Biochemistry 16*, 3080.
Erickson, B. W., & Merrifield, R. B. (1976) *Proteins 2*, 255.
Gold, M. H., & Segel, I. H. (1974) *J. Biol. Chem. 249*, 2417.
Gupta, R. K., Oesterling, M. M., & Mildvan, A. S. (1976) *Biochemistry 15*, 2881.
Hartley, B. S. (1970) *Biochem. J. 119*, 805.
Huiging, F., & Larner, J. (1966) *Proc. Natl. Acad. Sci. U.S.A. 56*, 647.
Jallon, J. M., & Cohn, M. (1970) *Biochem. Biophys. Acta 222*, 542.
Kemp, B. E., Graves, D. J., Benjamine, E., & Krebs, E. G. (1977) *J. Biol. Chem. 252*, 4888.
Krebs, E. G. (1972) *Curr. Top. Cell. Regul. 5*, 99.
Li, T. M., Mildvan, A. S., & Switzer, R. L. (1978) *J. Biol. Chem. 253*, 3918.
Maller, J. L., Kemp, B. E., & Krebs, E. G. (1978) *Proc. Natl. Acad. Sci. U.S.A. 75*, 248.
Merritt, E. A., Sundaralingam, M., Cornelius, R. D., & Cleland, W. W. (1978) *Biochemistry 17*, 3274.
Mildvan, A. S. (1970) *Enzymes, 3rd Ed. 2*, 445.
Mildvan, A. S., & Cohn, M. (1963) *Biochemistry 2*, 910.
Mildvan, A. S., & Cohn, M. (1966) *J. Biol. Chem. 241*, 1178.
Mildvan, A. S., & Engle, J. L. (1972) *Methods Enzymol. 26C*, 654.
Milner-White, E. J., & Watts, D. C. (1971) *Biochem. J. 122*, 727.
Miyamoto, E., Kuo, J. F., & Greengard, P. (1969) *J. Biol. Chem. 244*, 6395.
Miziorko, H. M., & Mildvan, A. S. (1974) *J. Biol. Chem. 249*, 2743.
Moll, G. W., Jr., & Kaiser, E. T. (1976) *J. Biol. Chem. 251*, 3993.
Moll, G. M., Jr., & Kaiser, E. T. (1977) *J. Biol. Chem. 252*, 3007.
O'Sullivan, W. J., & Cohn, M. (1966) *J. Biol. Chem. 241*, 3104.
Pomerantz, A. H., Allfrey, V. G., Merrifield, R. B., & Johnson, E. M. (1977) *Proc. Natl. Acad. Sci. U.S.A. 74*, 4261.
Reed, G. H., & Cohn, M., (1972) *J. Biol. Chem. 247*, 3073.
Stewart, J. M., & Young, J. D. (1968) *Solid Phase Peptide Synthesis*, W. H. Freeman, San Francisco, CA.
Sugden, P. H., Holladay, L. A., Reimann, E. M., & Corbin, J. D. (1976) *Biochem. J. 159*, 409.
Walsh, D. A., & Krebs, E. G. (1973) *Enzymes, 3rd Ed. 8*, 555.
Witt, J. J., & Roskoski, R., Jr. (1975) *Anal. Biochem. 66*, 243.
Yount, R. G., Babcock, D., Ojala, D., & Ballantyne, W. (1971) *Biochemistry 10*, 2484.
Zetterquist, O., Ragnarsson, U., Humble, E., Berglund, L., & Engstrom, L. (1976) *Biochem. Biophys. Res. Commun. 70*, 696.

Establishing the Misacylation/Deacylation of the tRNA Pathway for the Editing Mechanism of Prokaryotic and Eukaryotic Valyl-tRNA Synthetases†

Alan R. Fersht* and Colin Dingwall

ABSTRACT: The valyl-tRNA synthetases from *Bacillus stearothermophilus* and *Escherichia coli* have been shown to edit the mistaken activation of L-α-aminobutyrate (αBut) by first misacylating $tRNA^{Val}$ and then specifically deacylating the αBut-$tRNA^{Val}$. This pathway was established initially by rapid quenching and sampling experiments which detected the transiently formed αBut-$tRNA^{Val}$ on the addition of $tRNA^{Val}$ to the preformed and isolated E·αBut-AMP complex. The misacylation/deacylation pathway of editing was then shown to occur in the normal reaction in the steady state by isolation of the mischarged tRNA. For example, [^{14}C]-αBut-$tRNA^{Val}$ (*E. coli*) can be isolated from a steady-state reaction mixture containing [^{14}C]-αBut (0.9 mM), enzyme (71 μM), $tRNA^{Val}$ (72 μM), and ATP (8 mM), at the steady-state concentration predicted from the measured deacylation rate constant (50 s^{-1}) and the steady-state kinetic constants for the ATP/pyrophosphatase activity under these conditions. The same pathway appears to operate for the rejection of threonine by the eukaryotic valyl-tRNA synthetase since, on mixing the enzyme-bound threonyl adenylate and tRNA from yeast, transiently formed Thr-$tRNA^{Val}$ is observed and its deacylation rate constant estimated to be greater than 80 s^{-1}. The rate-determining step of the valyl-tRNA synthetase catalyzed deacylation of αBut-$tRNA^{Val}$ is shown to be different in nature as well as in magnitude from that of Val-$tRNA^{Val}$. The rate of the editing reaction is independent of pH between 6 and 7.8 and is unaffected by the addition of aminoacyl adenylate, whilst the rate of deacylation of Val-$tRNA^{Val}$ follows an ionization of pK_a = 8 and is decreased by the addition of aminoacyl adenylate. A unified scheme is presented that could account for the specificity in the deacylation reaction.

The fidelity of protein biosynthesis is far higher than expected from simple kinetic and thermodynamic arguments. One link in the synthetic chain where errors are likely to occur is at the aminoacylation of tRNA, for it is here that the cell has to distinguish between amino acids that are structurally very similar. The discrimination is accomplished by: (a) the aminoacyl-tRNA synthetases discriminating as precisely as possible between competing amino acids by the preferential binding of the cognate amino acid; (b) where necessary, the enzymes having evolved an *editing* function whereby mistakenly aminoacylated intermediates or products are hy-

† From the MRC Laboratory of Molecular Biology, Cambridge CB2 2QH, England. *Received June 13, 1978; revised manuscript received December 11, 1978.*

* Address from Sept 1978 to Sept 1979: Department of Biochemistry, Stanford University Medical Center, Stanford, CA 94305.

0006-2960/79/0418-1238$01.00/0